ISSN 1027-5495. Functional Materials, 25, No.2 (2018), p. 274-281.
doi:https://doi.org/10.15407/fm25.02.274

Galvanic ternary Fe–Co–W coatings: structure, composition and magnetic properties

I.Yu.Yermolenko, M.V.Ved', N.D.Sakhnenko, L.P.Fomina, I.G.Shipkova

National Technical University "Kharkiv Polytechnic Institute",
2 Kyrpychova St., 61002 Kharkiv, Ukraine

Received February 2, 2018

Principles of Fe–Co–W alloys electrodeposition from complex Fe (III) based citrate electrolytes are discussed. The effect of both current density and pulse on/off time on the quality, composition and surface morphology of the electrolytic alloys were determined. The application of pulsed electrolysis provides increasing tungsten content up to 13 at.%, at current efficiency of 70–75 %. Globular surface of Fe–Co–W coatings is caused by refractory metals incorporation, and crystalline and amorphous parts of structure are visualized by X-ray spectroscopy, including inter-metallic phases Co_7W_6, Fe_7W_6 along with α–Fe and Fe_3C. The coherent-scattering region size of the amorphous part is 2–8 nm. Magnetic characteristics of amorphous Fe–Co–W coatings were measured in dependence of deposition time. The conclusion was made that the content of magnetic phase in upper layers of coating is greater than in the bottom ones due to decreasing W atom concentration.

Keywords: coercive force, Fe–Co–W galvanic alloy, pulse electrolysis, magnetic properties.

Обсуждаются принципы электроосаждения сплавов Fe–Co–W из комплексных цитратных электролитов на основе Fe (III). Определены влияние плотности тока и длительности импульс/пауза на качество, состав и морфологию поверхности электролитических сплавов. Применение импульсного электролиза обеспечивает увеличение содержания вольфрама до 13 ат.% при эффективности процесса 70–75 %. Глобулярная поверхность покрытий Fe–Co–W обусловлена присутствием тугоплавких металлов, а результаты рентгеновской спектроскопии демонстрируют аморфно-кристаллическую структуру покрытий, включая интерметаллические фазы Co_7W_6, Fe_7W_6 вместе с α–Fe и Fe_3C. Размер зоны когерентного рассеивания аморфной части составляет около 2–8 нм. Проведены измерения магнитных характеристик аморфных покрытий Fe–Co–W в зависимости от времени осаждения. Показано, что содержание магнитной фазы в верхних слоях покрытия больше, чем в нижних, вследствие уменьшения количества вольфрама.

Гальванічні тернарні покриття Fe–Co–W: структура, склад і магнітні властивості. *І.Ю.Єрмоленко, М.В.Ведь, М.Д.Сахненко, Л.П.Фоміна, І.Г.Шипкова.*

Обговорюються принципи електроосадження сплавів Fe–Co–W з комплексних цитратних електролітів на основі Fe (III). Визначено вплив густини струму і тривалості імпульс/пауза на якість, склад і морфологію поверхні електролітичних сплавів. Застосування імпульсного електролізу забезпечує збільшення вмісту вольфраму до 13 ат.% при ефективності процесу 70–75 %. Глобулярна поверхня покриттів Fe–Co–W обумовлена присутністю тугоплавких металів, а результати рентгенівської спектроскопії демонструють аморфно-кристалічну структуру покриттів, зокрема інтерметаліди Co_7W_6, Fe_7W_6 разом з α–Fe і Fe_3C. Розмір зони когерентного розсіювання аморфної частини складає близько 2–8 нм. Проведено вимірювання магнітних характеристик аморфних покриттів Fe–Co–W залежно від часу осадження. Показано, що вміст магнітної фази у верхніх шарах покриття більше, ніж у нижніх, внаслідок зменшення вмісту вольфраму.

1. Introduction

Solving the applied problems in extending a range of functional materials predetermines interest in the electrolytic multicomponent alloys. Special attention is paid to the co-deposition of iron triad metals with refractory elements [1, 2]. Such coatings are interesting by the possibility of combining functional properties that exceed alloying metals. Spheres of multi-component coatings application are replacement of electrolytic toxic chromium and hardening of the surface [3–6], corrosion protection [7, 8], magnetic films with increased microhardness [9, 10], catalytic materials for heterogeneous red-ox processes [11, 12].

Utilization of the electrochemical methods for thin alloy coatings synthesis displays interactions in the chain "process parameters — composition and structure of the material — properties — functions — application". Of course, the advantage of above techniques for deposition thin-film multi-component systems is the possibility to flexibly control the content of components, rate of deposition, surface condition through the variation of the composition of electrolytes and regimes of polarization (static or pulse, reverse current or a decrease in potential) [13–15].

It should be noted that publications mainly reflect the binary Fe(Ni,Co)–Mo(W) alloys deposition and properties, but there are some positive results of the multi-component alloys deposition from the gluconate-chloride [3], citrate and citrate-ammonia [16], pyrophosphate [17], sulfate-citrate [18] electrolytes in galvanostatic and non-stationary mode. Addition of second magnetic component is able to change essentially magnetic characteristics of these alloys. In particular, alloys based on iron and cobalt are characterized by higher saturation magnetization than each of metals taken separately if Fe and Co concentrations are nearly equalled [19]. However, the main problem of the presented technologies remains the low content of refractory components and current efficiency [20, 21].

Given this, a study of electrolyte composition and electrolysis regimes influence on the composition, morphology and, consequently, properties of Fe–Co–W alloys is required.

2. Experimental

Ternary coatings were deposited onto planar samples out of two metals: copper and mild steel. Pretreatment of copper samples surface included mechanical polishing, degreasing, chemical etching in a mixture of the 50 % nitric and 50 % sulfuric acids, thorough washing with distilled water and drying. Pretreatment of steel samples included grinding, degreasing in a solution of sodium carbonate at 50°C, and washing, etching in a mixture of hydrochloric acid and sulfuric acid at a temperature of 20°C, and thoroughly washing in flowing water.

The Fe–Co–W coatings were formed from electrolytes of the composition, (*M*): iron(III) sulfate 0,05–0.075, cobalt sulfate 0.15–0.2, sodium tungstate 0.04–0.06, sodium citrate 0.4–0.5, sodium sulfate 0.15 and boric acid 0.1; the pH value was adjusted within the range 4.0–4.6 by addition of sulfuric acid or sodium hydroxide.

All electrolytes were prepared from analytically pure reagents, dissolved in a small amount of distilled water following by solution mixture in a certain sequence, based on the ionic equilibrium study results [22–24]. The acidity of solutions was controlled by pH-meter pH-150M with the glass electrode ESL-6307. Electrolyte temperature during deposition was varied in the range of 25–35°C.

The Fe–Co–W coatings were formed in two modes: (i) galvanostatic with the current density i 2–7 A/dm^2 and (ii) unipolar pulsed with current amplitude i of 2–6 A/dm^2 at an on-time (pulse duration) t_{on} = $1{\cdot}10^{-2}$–$2{\cdot}10^{-2}$ s and off-time (pause duration) t_{off} = $1{\cdot}10^{-2}$–$5{\cdot}10^{-2}$ s. As anode served plates of AISI 304 steel; the cathode-to-anode area ratio was 1:5, volume current density was kept at the level 2 A/dm^3.

Both the galvanostatic and pulse electrolysis were performed using dc and pulse current supply unit (ZY-100+12).

Current efficiency Ce (%) was determined by a gravimetric method on the assumption that metals in a deposited coating are in the completely restored state. Theoretical increase in mass as a result of electrodeposition was calculated according to the Faraday law taking into account the electrochemical equivalent of the alloy.

The chemical composition of the coatings was determined by energy dispersive X-ray spectroscopy (EDS) [25] on an Oxford INCA Energy 350 electron probe microanalysis integrated into the system of the SEM. The X-rays were excited by exposure of the samples to a beam of 15 keV electrons. The surface morphology of the deposits was studied with a Zeiss EVO 40XVP scanning electron microscope (SEM). Images were recorded by the registration of secondary elec-

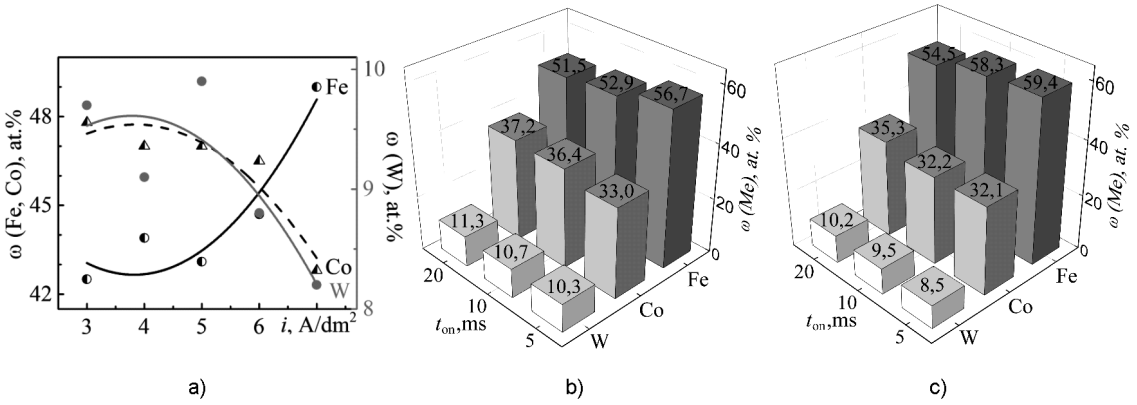

Fig. 1. Influence of electrolysis regime parameters on the composition of Fe–Co–W coatings obtained in (a) galvanostatic and (b, c) pulsed regimes; (b) i = 5 A/dm^2, t_{off} = 10 ms; (c) i = 6 A/dm^2, t_{off} = 10 ms.

trons (SEs) via scanning with an electron beam; this mode made it possible to study the topography with a high resolution and contrast ratio.

The surface morphology of thin films was studied by an atomic force microscopy AFM using a NT-206 scanning probe microscope. The tapping mode was conducted to measure samples surface morphologies. Scanning was performed by using the contact probe CSC-37 with a cantilever lateral resolution of 3 nm [26]. The scan area sizes were fixed at different scopes namely 39.9×39.9 μm, 20.0×20.0 μm, 10.0×10.0 μm and 5.0×5.0 μm and the height of the surface relief was recorded at the resolution of 256×256 pixels. For each sample, a variety of scans were obtained at random locations on the surface of thin films. In order to analysis the AFM images, all image data were converted into Surface Explorer software.

The structure of the deposits was examined by X-ray diffraction analysis using a diffractometer (DRON-2.0) in the emission of iron (cobalt) anode. X-ray patterns were recorded in discrete mode with a step $2\theta = 0.1°$ with the exposure at each point for 20 sec; operating voltage was 35 kV, and current 20 mA.

Magnetic characteristics were measured using vibrating sample magnetometer.

3. Results and discussion

Increasing concentration of citrate ions from 0.4 mol/dm^3 to 0.5 mol/dm^3 in solution at fixed Fe^{3+} content that's what expectedly increases the electrolyte pH from 4.3 to 4.55 respectively. The protonation of citrate anions decreases with pH, as well as degree of Fe^{3+} hydrolysis increasing, therefore ionic forms of complexing agents and ligand in the electrolytes are different. Consequently, the composition of particles discharged at the electrode varies, which effect the composition of coatings.

Fe–Co–W alloy deposition occurs by competitive reduction of iron, cobalt and tungsten [16, 22, 24]. The form of competition depends on the ratio of electrolyte components and electrolysis parameters. We observed a decrease in the cobalt and tungsten content in favor the iron portion in the alloy at all current densities (Fig. 1), if the ratio of electrolyte components concentration $c(Fe^{3+}):c(Co^{2+}):\ c(WO_4^{2-}):c(Cit^{3-})$ is 1:1.3:0.6:2.7. This occurs as a result of competitive reduction of alloying components from hetero-nuclear complexes. The cobalt content exceeds the iron portion in coatings deposited at current densities of 3–7 A/dm^2. A trend to gradually decreasing the cobalt content is observed with increasing current density (Fig. 1a). Iron and cobalt are co-deposited in the alloy in the ratio 1:1 at a current density of 6 A/dm^2. Further rising i_c promotes a significant increase in iron content at the expense of cobalt and tungsten. The refractory component content in the alloy varies within 8–10 at.% with tendency to decrease at rising current density. It should be noted that iron, cobalt and tungsten are co-deposited at the alloy in proportion to 4.5:5:1 respectively, if alloying metals ratio in the electrolyte is $c(Fe^{3+}):c(Co^{2+}):\ c(WO_4^{2-}) = 2.5:3:1$.

Tungsten content increases slightly (9–11 at.%) if the citrate concentration in the solution is 0.5 mol/dm^3 other things being equal. However, the trend to tungsten content decreasing with rising current density

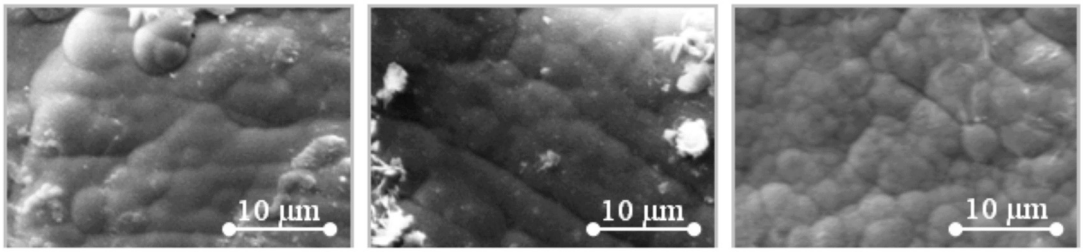

Fe 55.8; Co 38.4; W 5.8 a) | Fe 58.4; Co 35.4; W 6.2 b) | Fe 54.8; Co 32.7; W 12.5 c)

Fig. 2. The morphology and composition (at. %) of Fe–Co–W coatings deposited by (a) galvanostatic and (b, c) pulse modes; a) i = 3 A/dm^2; b) i = 3 A/dm^2, t_{on}/t_{off} = 50/50 ms; c) i = 5 A/dm^2, t_{on}/t_{off} = 20/20 ms.

is maintained. At the same time, the competitive reduction of iron and cobalt becomes more significant. The iron content in the coating increases to 59 at.% with a simultaneous decreasing in cobalt portion to 30 at.% when rising current density from 3 A/dm^2 to 7 A/dm^2.

The efficiency of galvanostatic deposition does not exceed 45 %, regardless of the electrolyte concentration. Increasing i_c to 7 A/dm^2 reduces the current efficiency to 27 % due to side reaction of hydrogen evolution. Deposited in stationary mode Fe–Co–W coatings have globular morphology of surface with a grain sizes of 2–6 μm (Fig. 2a). Coatings deposited in pulse mode contain expand amount of refractory metals, and are more uniform. The tungsten content in the coatings deposited by pulse current is of 6.2–12.5 at.% (Fig. 2b, c). On more developed surface of enriched with tungsten coatings, we can see agglomerates of spheroids (Fig. 2c). Time parameters of pulsed electrolysis are an effective tool for controlling the composition and nature of the coating surface. Prolong pulse at a fixed pause time contributes an increasing of cobalt and tungsten content in the alloy at studied current densities (Fig. 1b, c). At the same time, observed for the galvanostatic regime rising trend of iron content at the expense of cobalt and tungsten with increasing current density is preserved, as one can see on Fig. 1b, c.

The deposition efficiency increases almost twice when applying pulse current as compared with galvanostatic regime: at a current density of 3 A/dm^2 the current efficiency is 70–75 %, and at 4 A/dm^2 Ce decreases to 63–68 %, due to site hydrogen evolution reaction.

The roughness of galvanic coatings is the result of the alloy deposition and may serve as an additional indicator of the surface development as well as topography. The coating samples Fe–Co–W containing refractory components of 10–12 at.% deposited on mild steel were studied by AFM analysis. The substrate of mild steel is characterized by evenly surface (Fig. 3a) with roughness R_a = 0.008 and R_q = 0.011. However, the structure of surface is not ordered. The cross section profile between markers 1 and 2 indicates that the grain sizes are in the range of 2–3 μm as one can see from Fig. 3a.

The data of the AFM analysis demonstrate the globular surface of the Fe–Co–W coatings. Wherein larger spheroids of size of 2.5–3.5 μm is formed with a smaller grains of sizes of 0.2–0.5 μm as one can see from Fig. 3b. It was found earlier [8] that globular structure of the surface is caused by the refractory metals incorporation into alloy. Such composition and character of the surface are favorable for increasing microhardness, corrosion resistance, and catalytic activity of the material [3, 12]. Surface roughness parameters at scanning area 5×5 μm are defined as R_a = 0.06 and R_q = 0.07 that much higher than those for the substrate and shows substantial development of the surface.

Figure 4 shows the results of X-ray diffraction analysis and phase structure for Fe–Co–W coatings of composition (in terms of metal) at.%: Fe — 54, Co — 36, W — 10, which deposited on a copper substrate, a thickness of coating is of 30 μm. The X-ray diffraction pattern indicates an amorphous-crystalline structure of the Fe–Co–W alloy (Fig. 4). We can see some lines of copper substrate, and lines corresponding to intermetallic phases Co_7W_6 and Fe_7W_6, as well as α–Fe and cementite Fe_3C at diffraction patterns. Besides, a low halo with width about 10° is detected at angles 2θ 50–55° (Fig. 4), that corresponds to amorphous

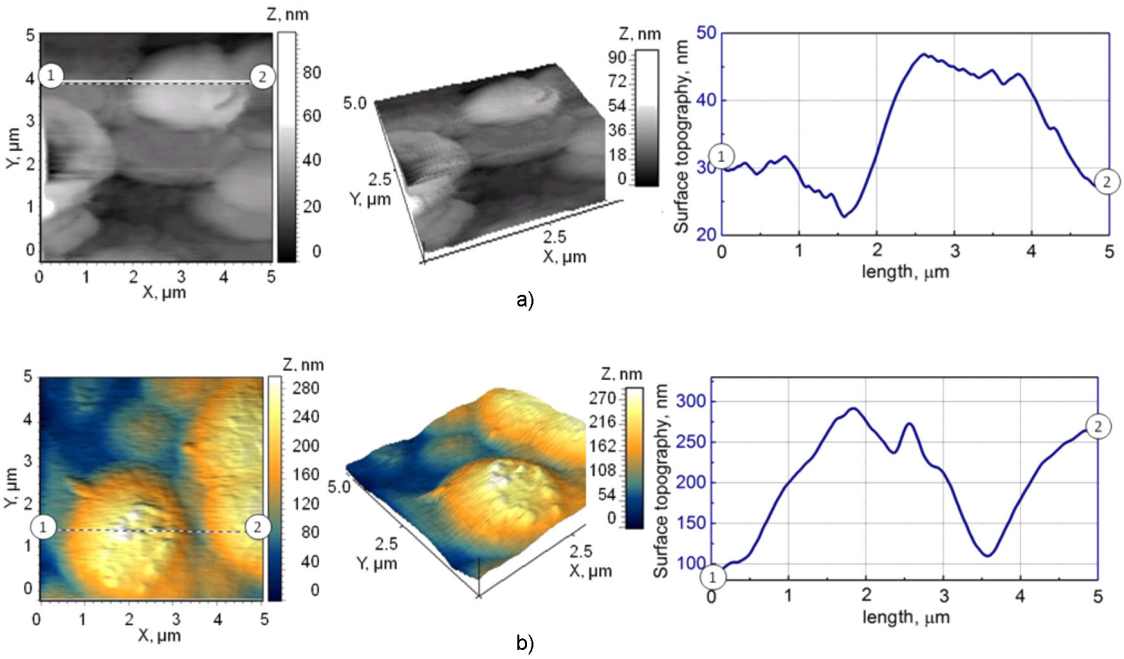

Fig. 3. 2D- and 3D maps of the surface and cross section profile between markers 1 and 2 for (a) mild steel substrate and (b) Fe–Co–W coating deposited in pulse mode at current density 4 A/dm^2; t_{on}/t_{off} = 10/10 ms; plated time 30 min. Scan area 5.0×5.0 μm.

structure. The crystallite size of the amorphous part is 2–8 nm.

Additional information relating to coating structure can be obtained by analysis of magnetic properties parallel with coating compositions. Four type of the samples obtained by pulse mode differing by deposition period (1, 3, 5 and 10 min) were investigated.

XRD data evidenced that these coatings were X-ray amorphous. Characteristics of these samples are presented in the Table as well as in the Fig. 5.

It can be seen from the table that the content of components change during electrodeposition process. Tungsten atomic concentration decreases with deposition time.

Magnetic properties change too. The magnetic moments referred to surface unit (M/S) increase nonlinearly in dependence of deposition period (Fig. 5). We can see that the rate of magnetic moment change increases. It indicates that inhomogeneous distribution of ferromagnetic phases (FM) throughout the coating cross-section for the thickest samples is to be observed. Quantity of FM phase is the largest in upper layers of coatings. Qualitatively it corresponds to W content changes (decreasing) under thickness growth.

At the same time the quantitative estimates of alloy magnetization that has been

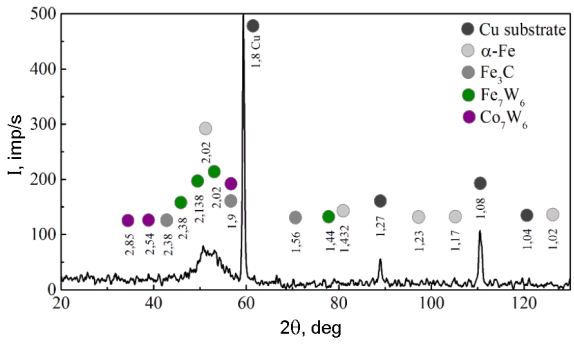

Fig. 4. X-ray diffraction patterns for deposit Fe–Co–W.

carried out on the assumption that the alloy was a homogeneous mixture of two types of magnetic atoms and one type of nonmagnetic ones packaged in a random manner (a model of dense random packing of hard spheres) gave higher values than those that can be calculate on the basis of experimental data on the magnetic moment and the thickness of the coatings. Thus, for an amorphous alloy the value of the spontaneous magnetization is usually associated with the average magnetic moment of the atom as [27]:

$$M_S = \tilde{\mu} \cdot N_A \cdot \rho \cdot \beta / A, \qquad (1)$$

where N_A is Avogadro's number, ρ is the average density of the alloy, β is a constant,

Table. Magnetic characteristics and composition of Fe–Co–W alloys

No.	t, min	ω (M), wt.%			M/S, 10^{-7} emu/cm^2 ($H_{min\,=\,1000\ Oe}$)	H_c, Oe	ω (M), at.%		
		Fe	Co	W			Fe	Co	W
1	1	38.6	30.8	30.6	155621	70	50.0	37.9	12.1
2	3	38.4	35.1	26.5	564064	70	48.1	41.8	10.1
3	5	40.0	33.1	26.9	1208710	60	50.3	39.5	10.3
4	10	42.1	33.8	24.1	2719596	30	51.7	39.4	9.0
					2840467 (H_{max} = 5000 Oe)				

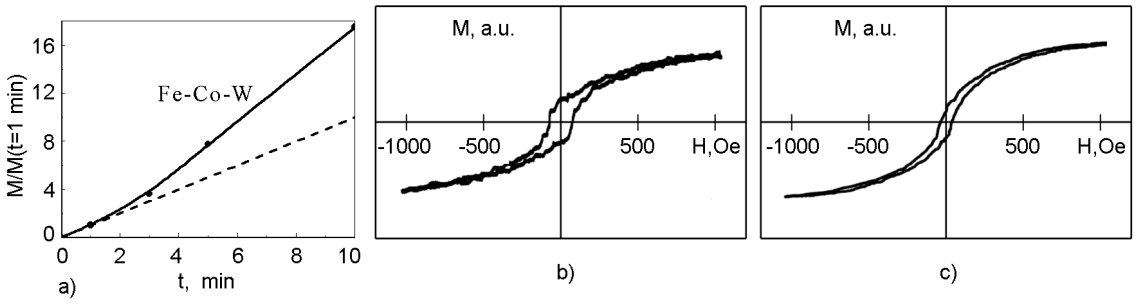

Fig. 5. Magnetic characteristics of amorphous Fe–Co–W coatings; (a) relative change in the magnetic moment of the coatings with deposition time increasing; (b, c) — hysteresis loops. Deposition time is (b) 1 min; (c) 10 min.

and A is the average molar mass for a given composition alloy. The average magnetic moment is determined only by the magnetic moment of magnetic atoms and their concentration in the alloy:

$$\tilde{\mu} = c_{Fe} \cdot \mu_{Fe} + c_{Co} \cdot \mu_{Co}. \qquad (2)$$

Estimates of the spontaneous magnetization in accordance with the data of the table relating to atomic concentration of the components and the calculated values of the average alloy density (~9.4–9.8 g/cm^3 for W-containing alloys) and the average molar mass (70 g/mol) at $\beta \approx 1$ give the magnetization values that are equaled to ~1320–1380 G for alloys with tungsten. The magnetization values calculated using the experimentally determined magnetic moments in magnetic fields where a state close to magnetic saturation is reached was less than 680 G. Such a strong discrepancy between calculations and experiment may be due to the fact that the structure of real amorphous coatings is not the same as in a system of uniformly distributed heterogeneous atoms. It is known [19, 28] that crystalline alloys of similar compositions in the state of thermodynamic equilibrium consist of nanodispersed ferromagnetic phases (solid solutions of W in iron and cobalt) and weak-magnetic (paramagnetic) phases such as intermetallides like μ phase of (Co, Fe)$_7$W$_2$(Co, Fe, W)$_4$. It can be assumed that in the nonequilibrium electrodeposition process clusters with a short-range order similar to that of number of intermetallic nonmagnetic compounds are formed in the alloy too. It leads to decrease of alloy saturation magnetization. This assumption is supported by diffractograms measured for coatings of similar compositions, however prepared not in the pulsed mode, but in the galvanostatic regime (Fig. 4) where crystalline phases are already detected. Phase analysis shows the presence of Fe$_7$W$_6$, Co$_7$W$_6$ intermetallides and solid solution of α–Fe as mentioned above.

Hysteresis loops of Fe–Co–W alloys of different deposition period are shown in Fig. 5. The shape of the hysteresis loop varies insignificantly with increasing deposition time, but a gradual decrease in the coercive force H_C from 70 Oe to 30 Oe is observed (see Table). Coercive force of amorphous materials is known to be determined by the same factors as ones of crystalline materials. When magnetization reversal is realized by displacement of domain walls, various variants of wall fixing on the different kinds of inhomogeneities should

be considered. For instance, in amorphous strips obtained by melt quenching the total value of the coercive force contains contributions from fluctuations of the exchange interaction and local anisotropy, chemical short-range order and surface irregularities. In the alloys with a non-zero magnetostriction constant there is a contribution of elastic stress inhomogeneities inside the material. The last two factors make the largest quantitative contribution to the total coercive force value. The formulas for calculating each component are quite complex [29]. But it was shown that the contribution of the surface component to the H_C value is directly proportional to the ratio of the local roughness to the thickness of the layer. Therefore, when the thickness increases and the relief remains that existed before, the coercive force should decrease. The inhomogeneities of the elastic stresses are related to the existence of a free volume and this component of the coercive force is proportional to the density of such regions. It should be expected that the same, but more pronounced factors control the coercive force in amorphous electrodeposited coatings. So, samples under study have a highly developed surface relief (Fig. 3). The release of hydrogen during electrodeposition process leads to the appearance of regions of free volume and therefore to not uniform stress fields. At the same time Fe–Co–W coatings have higher H_C values than amorphous alloys containing P, B, and Si elements as a non-magnetic component. Probably, in our case the large clusters that have composition order like paramagnetic intermetallide W phases play noticeable role in magnetization reversal along with roughness and free volume.

4. Conclusions

Thus ternary Fe–Co–W alloys with micro-globular surface of different composition were deposited by direct and pulse current from citrate Fe (III) based electrolyte. Current density and time parameters of pulse electrolysis are shown to be affective tools to control the refractory metals content and electrolysis efficiency.

Micro-globular surface of Fe–Co–W alloys is caused by tungsten incorporation. The amorphous-crystalline structure of deposits with crystallite sizes of the amorphous part 8 nm was found.

Magnetic characteristics of amorphous Fe–Co–W coatings were measured in dependence of deposition time. The conclusion was made that the content of magnetic phase in upper layers of coating is greater than in the bottom ones due to decreasing W atom concentration.

References

1. N.Tsyntsaru, H.Cesiulis, M.Donten et al., *Surf. Eng. Appl. Electrochem.*, **48**, 491 (2012).
2. G.Yar-Mukhamedova, M.Ved', N.Sakhnenko et al., *Appl Surf. Sci.*, **383**, 346 (2016). doi:http://dx.doi.org/10.1016/j.apsusc.2016.04.046.
3. H.Capel, P.H.Shipway, S.J.Harris, *Wear*, **255**, 917 (2003), doi:10.1016/S0043-1648(03)00241-2.
4. M.V.Ved', M.D.Sakhnenko, H.V.Karakurkchi et al., *Mater. Sci.*, **51**, 701 (2016), doi:10.1007/s11003-016-9893-5.
5. H.Feng-jiao, L.Jing-tian, L.Xin, H.Yu-ning, *Trans. Nonferrous Met. Soc. China*, **14**, 901 (2004).
6. Salt Liwen Ma, Xiaoli Xi, Zuoren Nie et al., *Int. J. Electrochem. Sci.*, **12**, 1034 (2017), doi:10.20964/2017.02.37.
7. N.Tsyntsaru, A.Dikusar, H.Cesiulis et al., *Powder Metall. Met. Ceram.*, **48**, 419 (2009).
8. Y.S.Yapontseva, A.I.Dikusar, V.S.Kyblanovskii, *Surf. Eng. Appl. Electrochem.*, **50**, 330 (2014), doi:10.3103/S1068375514040139.
9. E.Gomez, E.Pellicer, E.Valles, *J. Electroanal. Chem.*, **517**, 109 (2001).
10. E.Gomez, E.Pellicer, E.Valles, *J. Electroanal. Chem.*, **568**, 29 (2004), doi:10.1016/j.jelechem.2003.12.032.
11. V.S.Kublanovsky, Yu.S.Yapontseva, *Electrocatalysis*, **5**, 372 (2014), doi:10.1007/s12678-014-0197-y.
12. M.Glushkova, T.Bairachna, M.Ved, M.Sakhnenko, in: MRS Proc., **1491**, mrsf12-1491 (2013).
13. I.Y.Yermolenko, M.V.Ved, N.D.Sakhnenko, Y.I.Sachanova, *Nanoscale Res. Lett.*, **12**, 352 (2017), doi:10.1186/s11671-017-2128-3.
14. M.V.Ved', N.D.Sakhnenko, A.V.Karakurchi, S.I.Zyubanova, *Russ. J. Appl. Chem.*, **87**, 276 (2014), doi:10.1134/S1070427214030057.
15. D.Z.Grabco, A.I.Dikusar, V.I.Petrenko, E.E.Harea, *Surf. Eng. Appl. Electrochem.*, **43**, 11 (2007).
16. A.V.Karakurkchi, M.V.Ved', N.D.Sakhnenko, I.Yu.Ermolenko, *Russ. J. Appl. Chem.*, **88**, 1860 (2015), doi:10.1134/S107042721511018X.
17. N.Elezovic, B.N.Grgur, N.V.Krstajic, V.D.Jovic, *J. Serb. Chem. Soc.*, **70**, 879 (2005).
18. E.Gomez, E.Pellicer, X.Alcobe, E.Valles, *J. Solid State Electrochem.*, **8**, 497 (2004), doi;10.1007/s10008-004-0495-z.
19. R.Bosart, Ferromagnetism, Inostrannaya Literatura, Moskva (1956) [in Russian].
20. F.I.Danilov, I.V.Sknar, Yu.E.Sknar, *Russ. J. Electrochem.*, **50**, 293 (2014).
21. D.P.Weston, S.J.Harris, P.H.Shipway et al., *Electrochim. Acta*, **55**, 5695 (2010).

22. M.D.Sakhnenko, M.V.Ved', I.Yu.Ermolenko et al., *Mater. Sci.*, **53**, 680 (2017), doi:10.1007/s11003-017-0009-7.
23. N.Cirovic, P.Spasojevic, L.Ribic-Zelenovic et al., *Sci. Sintering*, **47**, 347 (2015), doi:10.2298/SOS1503347C.
24. I.Y.Yermolenko, M.V.Ved', A.V.Karakurkchi et al., *The Issues Chem. Chemical Technol.*, **2**, 4 (2017).
25. I.F.Mikhailov, A.A.Baturin, A.I.Mikhailov, E.A.Bugaev, *Instruments and Exp.Techniques*, **56**, 84 (2013).
26. M.Labardi, M.Allegrini, M.Salerno et al., *Appl. Phys.*, **59**, 3 (1994).
27. K.Sudzuki, X.Phydzimori, K.Hasimoto, Amorphous Metals, Metallurgy, Moscow (1987) [in Russian].
28. A.F.Guillermet, Z.Metallkde, *Bd.79 H.*, **10**, 633 (1988).
29. Ph.Ye.Lyuborsky, Amorphous Metal Coatings, Metallurgy, Moscow (1987) [in Russian].